Neutrophil Extracellular Traps Facilitate Sympathoexcitation After Traumatic Brain Injury Via HMGB1/AP1 Signaling Pathway

Kaixin Zhu
Changzheng Hospital: Shanghai Changzheng Hospital
Xiaoxiang Hou
Changzheng Hospital: Shanghai Changzheng Hospital https://orcid.org/0000-0002-9405-4995
Xiaolin Qu
Shanghai Changzheng hospital
Wen Chen
Changzheng Hospital: Shanghai Changzheng Hospital
Kun Chen
Changzheng Hospital: Shanghai Changzheng Hospital
Yelei Zhang
Changzheng Hospital: Shanghai Changzheng Hospital
Haoxiang Xu
Changzheng Hospital: Shanghai Changzheng Hospital
Junyu Wang
Changzheng Hospital: Shanghai Changzheng Hospital
Liquan Lv
Changzheng Hospital: Shanghai Changzheng Hospital
Danfeng Zhang
Changzheng Hospital: Shanghai Changzheng Hospital
Lijun Hou (lijunhoucz@126.com)
Changzheng Hospital: Shanghai Changzheng Hospital

Research

Keywords: Traumatic brain injury, Sympathetic excitation, NETs, Microglial activation, HMGB1, AP1

Posted Date: December 6th, 2021

DOI: https://doi.org/10.21203/rs.3.rs-1102135/v1

Abstract

Background: Traumatic brain injury (TBI) usually accompanies with sympathetic excitation, and paradoxical sympathetic hyperactivity (PSH) may be detrimental to the prognosis of TBI sufferers. Neutrophils can form neutrophil extracellular traps (NETs) to get involved in the neuroinflammation after TBI. As an important form of NETs, HMGB1 were found to activate the expression of AP1, which can increase the formation of IL-1β in microglia. Considering that IL-1β is able to regulate sympathoexcitation, it is reasonable to infer that HMGB1/AP1 signaling plays an important role in sympathoexcitation after TBI.

Methods: In this present study, rat model with diffuse axonal injury (DAI) was established. The existance of NETs and the expression level of HMGB1/AP1/IL-1β in the paraventricular nucleus (PVN) after DAI were examined by immunofluorescence and Western blot (WB). The role of HMGB1/AP1 in the activation of microglia, secretion of IL-1β and sympathoexcitaiton were identified in vitro. Moreover, stereotaxic injection of anti-HMGB1 or HMGB1 was conducted to further validate the effect of HMGB1/AP1 pathway on sympathoexcitation after TBI.

Results: The indicators of sympathoexcitation, including mean arterial pressure and serum catecholamine, increased and peaked at 72 hours after TBI. The formation of NETs was observed in PVN after injury, whereas, no NETs were found in the control group. And meanwhile, levels of NETs in PVN were higher than that in the para-PVN tissues after the injury. *In vitro* experiments showed that HMGB1 can promote the activation of microglia as well as increase the expression of AP1 and IL-1β. *In vivo* experiments suggested HMGB1 have an impact on the expression of AP1 and IL-1β in the PVN, and further controlling the sympathoexcitation after TBI.

Conclusion: NETs might mediate sympathoexcitation after TBI through microglial activation in the PVN in a HMGB1/AP1/IL-1β dependent way.

Introduction

Traumatic brain injury (TBI) is defined as a disruption of normal brain function caused by an external physical force and it is a major cause of disability and mortality worldwide [1]. TBI is often followed by various complications that further exacerbate the damage following TBI, such as cerebrospinal fluid leakage, meningitis, visual impairment, paroxysmal sympathetic hyperactivity (PSH), psychosocial disorders, and so on. PSH, a special form of sympathoexcitation, has drawn considerable attention for its damage to patients after TBI. It is characterized by increased temperature, heart rate and blood pressure, and ecphysesis, which is reported to reduce the survival rate, prolong the hospital stay and contribute to poor outcomes [2–4]. Thereby, it is rational to control sympathoexcitation in an appropriate way to curb its deleterious outcomes

There are numerous pathological hypotheses explaining PSH after TBI. It is widely accepted that the disconnection of cerebral inhibitory pathways from excitatory centers in the cauda of the brain plays an

important role in the process [5]. Briefly, when the signal from the higher regulatory center is inhibited or blocked, or the lower regulatory center is abnormally activated, PSH occurs, leading to a series of typical clinical symptoms [6]. The paraventricular nucleus (PVN) of the hypothalamus is the core site for regulating sympathoexcitation in a variety of clinical diseases [7] and might play a part in the pathogenesis of PSH after TBI.

After TBI, the immune cells, especially neutrophils accumulating at the injured epicenter could clear the necrotic tissue and kill various pathogens [8]. Neutrophils are primarily bactericidal by phagocytosis or release of various bactericidal particles. However, recently, it has been found that neutrophils could also exert their effect in a special way named neutrophil extracellular traps (NETs). NETs are net-like complexes consisting chromatin DNA, histones, and neutrophil granule proteins located in the extracellular space [9].

High-mobility group box 1 (HMGB1), as one of the main components of NETs, is found to be potentially associated with sympathoexcitation in cardiovascular diseases [10]. Meanwhile, HMGB1 is an agonistic ligand for the RAGE receptor, which is a pattern recognition receptor highly expressed on cell membranes of monocytes such as microglia. RAGE can promote microglial activation and proliferation, as well as mediate inflammatory responses within microglia in pathological conditions such as TBI, ischemic brain injury (IBI), Alzheimer's disease (AD) [11, 12]. In aortic endothelial cells, activation of RAGE can further promote the expression of AP1 [13], a transcription factor closely related to the transcription of inflammatory cytokines such as IL-1β [14, 15]. However, it is not clear whether this regulatory relationship exists in microglia of PVN. IL-1β is one of the key cytokines of inflammatory response after TBI and accounts for sympathetic excitability in many cases [16–18]. Therefore, we speculate that neutrophils infiltrate into the PVN after TBI and form NETs. HMGB1 in NETs acts as a ligand to activate RAGE receptor on microglia, which leads to the activation of microglia and expression of IL-1β through RAGE/AP1 pathway, finally contributing to sympathoexcitation. The role of NETs in PSH after TBI has been preliminarily studied in our previous article [19], and mechanism of HMGB1/AP1 pathway in sympathoexcitation has been investigated in the present study.

Material And Method

2.1 Animals

Sprague Dawley (SD) rats, male, 8 weeks old, weighing 230-250g, were provided by the Animal Experiment Center of the Naval Medical University. All experimental operations strictly abided by the Guide for the Care and Use of Laboratory Animals published by US National Institutes of Health (NIH publication No.85-23, revised 1996) and were approved by Animal Care and Use Committee of the Naval Medical University. During this process, efforts were made to minimize the pain and number of animals used.

2.2 Experimental design

2.2.1 To explore the formation of NETs and the law of sympathetic excitability after TBI, 75 male SD rats were randomly divided into control group (n = 30) and experimental group (n = 45). After DAI attack, 30 surviving rats were randomly selected from the experimental group for further experiments. The experimental procedure of the control group was consistent with that of experimental group, except for the DAI attack. Both groups were equally divided into 5 subgroups (n=6) according to different time points (24 hours, 48 hours, 72 hours, 120 hours, 168 hours). The heart rate variability (HRV), arterial blood pressure (BP) and serum catecholamine (CA) concentration were measured and analyzed at the different time points. Brain tissue was harvested for pathological observation, including immunohistochemical staining of β-amyloid precursor protein (β-APP), HMGB1 and AP1, dual immunofluorescence staining of CitH3-MPO and Western bolt of IL-1β.

2.2.2 In *in vitro* experiment, cells were divided into solvent control group and HMGB1 group. Cells in HMGB1 group were added with different concentrations of HMGB1 recombinant protein (10ng/ml, 50 ng/ml, 100 ng/ml, Novoprotein, Shanghai, China), and those in control group were added with the same amount of PBS buffer solution instead. Subsequently, cells were incubated for 24 hours and then collected for detection.

2.2.3 To further confirm the role of HMGB1/AP1 pathway in sympathetic excitability *in vivo*, 30 male SD rats were randomly divided into sham group (n = 12) and DAI group (n = 18). After DAI attack, 12 surviving rats from DAI group were further randomly divided into DAI+Anti-HMGB1 group (n=6) and DAI+NS (normal saline) group (n=6). Rats in sham group were further randomly divided into sham+HMGB1 group (n=6) and sham+NS group (n=6). The procedure done for rats in sham group was consistent with that of DAI group except for the attack. In 2 DAI subgroups, anti-HMGB1() or NS were injected into the PVN 24 hours after attack. Meanwhile, the 2 sham subgroups were injected with HMGB1 or NS 24 hours after sham operation. HRV, blood pressure and serum CA, AP1, IL-1β in PVN were analyzed 72 hours after operation.

2.3 Cell culture and processing

HMC3 microglial cells were purchased from the cell bank of the Chinese Academy of Sciences in Shanghai and seeded on culture format in MEM (Fuheng Biotechnology, phm01, China) supplemented with 1% PBS and 10% fetal bovine serum (FBS, Biological Industries). Cultures were maintained at 37 °C in a 5% CO_2 humidified atmosphere for 3 days and then collected for further processing.

To process HMC3 cells, they were seeded on 12-well format in culture medium with different concentration of HMGB1 recombinant protein (0ng/ml, 10ng/ml, 50 ng/ml, 100 ng/ml). After culture for 24 hours, morphologic change of cells was observed.

2.4 DAI and sham-injury

DAI and sham-injury were conducted according to a standard protocol as previously described [20]. Rats were anesthetized with isoflurane and fixed on the DAI device. The head was rotated about 75 degrees

(4.68ms, 1.6 × 1.815 rad/s) on the coronal plane, and moved 1.57cm (4.66ms, 3.4 × 102 cm/s) horizontally to realize the angular/linear acceleration and deceleration injury of the brain. Then the tongue of the rat was pulled out with ophthalmic forceps to prevent suffocating. Rats in the control group received anesthesia and were fixed on the same device without the strike.

2.5 Stereotaxic injection administration

After anesthesia with inhaled isoflurane, rats were placed in an animal stereotaxic apparatus (ALCBIO, ALC-H, China). The injection was located −1.8 mm anteroposterior, ±0.4 mm mediolateral, −7.7 mm dorsoventral below the surface relative to bregma. The coordinates were determined based on the atlas of rats [21]. A total of 0.2 μL NS, anti-HMGB1 or HMGB1 was injected into the PVN using a 1-μl microsyringe (GAOGE, Shanghai, China) at a speed of 0.1uL/min. The needle was carefully pulled out after holding it in place for 10 min.

2.6 HRV Monitoring

The HRV analysis system (ALCBIO, MPA-HBBS, Shanghai, China) was used to record the rats' electrocardiogram (ECG). Animals were anesthetized with inhaled isoflurane in the supine position. The electrode and rat limbs were sterilized with 75% alcohol. The white, black and red recording needles were inserted into the right forelimb, right hindlimb and precordial area subcutaneously. When P, QRS, T and other wave groups can be clearly identified with no interference signal, ECG signal data were recorded for 15 to 30 minutes each time. The frequency domain and time domain were performed with the software of the system.

2.7 Intravascular cannulation

The anesthetized rat was fixed on a constant temperature operating table in the supine position. Polyethylene Catheters (consisting of 5-cm PE-10 tubing tightly bonded to 15-cm PE-50 tubing) were placed in the abdominal aorta by insertion through the femoral artery for the measurement of BP. The catheters were subcutaneously tunneled and exteriorized at the back of the neck between the scapulae. Finally, the catheters were flushed with heparin (0.2 ml, 200 IU/ml) and plugged with stainless steel pins. Incisions were closed by surgical sutures. BP was measured on freely-moving conscious rats 24 hours following the surgery. Briefly, the arterial catheter was connected to a transducer connected with the BP recorder (ALCBIO, ALC-MPA, Shanghai, China). During the process, heparin (20 IU/ml, 0.5 ml/h) was continuously pumped into the catheter to prevent blockage.

2.8 Enzyme-Linked Immunosorbent Assay (ELISA)

Levels of serum CA and IL-1β in culture medium were measured using commercially available CA (JINGMEI Biotechnology, China) and IL-1β (JINGMEI Biotechnology, China) ELISA-KIT according to the manufacturer's instruction. Each ELISA analysis was conducted in triplicate. To quantify CA and IL-1β levels, the absorbance of samples was read and analyzed at 450 nm on a spectrophotometric plate reader (BioTek Synergy HT, Winooski, USA).

2.9 Western Blot (WB)

The protein concentration was measured with the BCA kit (E112-01, Vazyme, Nanjing, China) according to the manufacturer's instructions. Lysates were applied to a 10% SDS-PAGE gel and then transferred to PVDF membrane. The membrane was blocked and incubated with primary antibody against IL-1β (1:1000, Zen Bio, 511369, China) or AP1(1:1000, CST, 60A8, USA) overnight at 4℃, followed by incubation with secondary antibodies (1:5000, ThermoFisher Scientific, USA) for 2 hours at room temperature. Finally, the protein bands were visually detected and analyzed. Tubulin served as a loading control.

2.10 Real-Time Fluorescent Quantitative PCR (RT-qPCR)

Total RNA from cell lysates was extracted out and reverse-transcripted into cDNA (321392, Promega, Beijing, China). The sequences of the primer pairs were as follows: C-AP1-F: CCTTGAAAGCTCAGAACTCGGAG; C-AP1-R: TGCTGCGTTAGCATGAGTTGGC; IL-1β-F: CCACAGACCTTCCAGGAGAATG; IL-1β-R: GTGCAGTTCAGTGATCGTACAGG. Then RT-qPCR was performed (Applied Biosystems). Cycle time values were measured as a function of GAPDH mRNA levels in the same lysates.

2.11 Immunofluorescence

The brain sections were permeabilized with 0.4% Triton X-100 for 10 minutes and rinsed three times in PBS solution for 5 minutes each time. After washing, the brain sections were blocked for 35 minutes in 2% bovine serum albumin, and then incubated overnight at 4 °C with primary antibodies: CitH3(1:100, Abcam, ab5103, USA) and MPO (1:50, Abcam, ab90810, USA). Subsequently, the sections were washed with PBS and incubated with appropriate FITC (1:50, Boster, China)-conjugated secondary antibodies for 2 hours at room temperature, followed by counterstain with 4',6'- diamidino-2-phenylindole (DAPI, Invitrogen) for 6 minutes. After the above procedures, the sections were observed and analyzed by ImagePro Plus 6.0.

2.12 Histopathology and Immunohistochemistry

Anesthetized rats were perfused with PBS (0.01 M, pH 7.40, 4 °C) and then perfused with 4% paraformaldehyde (PFA) solution (pH 7.40, 4 °C) transcardially. The brains were dissected in 4% PFA solution for fixation (24 h, 4 °C) and subsequently embedded in paraffin. Sections of 3μm to 5μm thickness were cut and stained with hematoxylin and eosin to observe the brain injury.

Frozen sections were subjected to immunostaining. Briefly, the sections were rehydrated with an ethanol gradient, treated with 0.3% hydrogen peroxide and 0.3% Triton X-100 for 30 minutes, followed by three washes with PBS. The sections were then incubated at 4℃ overnight with anti-β-APP (1:500, Abcam, ab32136, USA), anti-HMGB1(1:50, Zen Bio, 22773, China) or anti-AP1(1:200, CST, 60A8, USA) antibodies diluted in PBS containing 5% normal goat serum. On the second day, the sections were washed three times with PBS and incubated with the appropriate secondary antibodies (1:5000, ThermoFisher

Scientific, USA) for 30 minutes at 37°C. After another wash for three times, the sections were incubated with SABC. Subsequently, the samples were washed three times with PBS and reacted with DAB. Finally, all sections were counterstained with hematoxylin for 2 minutes, then dehydrated and coverslipped.

2.13 Statistical Analysis

Results are expressed as mean ± SEM. Data were analyzed using the Mann–Whitney U and two-way ANOVA tests. Values of P <0.05 were considered statistically significant and marked as *P < 0.05, **P < 0.01, ***P < 0.005.

Results

3.1 General information

In the experimental group, 8 of 45 rats died. After the injury, both of the breath rate and heart rate of all rats increased. Ten rats exhibited limb twitch, otorrhagia or epistaxis. Rats in the control group all survived. There was no difference in the diet, daily activities, or growth processes between the two groups.

3.2 Pathological changes of brain after DAI

Results of Hematoxylin-eosin (HE) staining showed diffuse subarachnoid hemorrhage in rats of the experimental group, which was not found in those of the control group (fig 1). Degeneration and necrosis were detected in the cortex, subcortical, corpus callosum, hippocampus and hypothalamus (fig 2) of rats in the experimental group.

It was reported that the level of intracellular β-App increased in brain tissue after DAI [40]. Results of immunohistochemistry suggested that β-APP expression in the hypothalamus and hippocampus of the experimental group was higher than that of the control group, and some nuclei were pyknotic and deformed in the DAI group (fig 3 A-D). Analysis of integral optical density (IOD) indicated that β-APP's expression in the experimental group was significantly increased in the hypothalamus (15459.93±457.65 vs 2244.87±860.78, P<0.001) and hippocampus (10564.04±1955.05 vs 3784.63±688.99, P<0.01) (fig 3E) compared with that of the control group.

3.3 Alteration of sympathoexcitation after DAI

3.3.1 Mean arterial pressure (MAP)

MAP of the experimental group began to increase within 24 hours after stroke and reached the peak at 72 hours, which was significantly higher than that of the control group (121.54 ± 1.33 mmHg vs 107.78 ± 1.56 mmHg, P < 0.001). Within 168 hours after stroke, MAP of the experimental group was higher than that of the control group (Fig 4A), which was stable all the way.

3.3.2 HRV

HRV can be expressed by standard deviation of normal-to-normal RR intervals (SDNN). The decrease of SDNN indicated the enhancement of sympathetic excitability [41, 42]. SDNN of rats in the experimental group decreased after injury and reached the lowest value at 72 hours, which was significantly lower than that of the control group (5.22 ± 0.71 ms vs 6.47 ± 0.70 ms, $P < 0.05$) (fig 4B). The SDNN of rats in the control group was stable at each time point.

3.3.3 Serum CA

Serum CA content (ng/ml) of rats in the experimental group peaked at 72 hours after the injury, which was significantly higher than that of the control group (508.50 (493.20, 607.80) ng/ml vs 333.45 (322.60, 348.35) ng/ml, $P < 0.01$) (fig 4C). The content of serum CA in the control group decreased 48 hours after sham operation.

3.4 DAI promoted the formation of NETs and activated HMGB1/AP1 pathway

Immunostaining for myeloperoxidase (MPO, green), citrullinated histone H3 (CitH3, red) and DAPI (blue) was performed to detect the formation of NETs 72 hours after DAI attack according to previous research [22]. In the experimental group, the levels of NETs in the PVN were higher than that in para-PVN tissue. In the control group, there was no formation of NETs within the PVN or para-PVN tissue (fig 5).

At 72 hours after DAI, immunohistochemistry analysis showed that the expressions of HMGB1 and AP1 were significantly increased in the PVN compared with those of the para-PVN tissue (IOD of HMGB1, 12405.47±1817.76 vs 7760.15±851.90, $P<0.05$) (IOD of AP1, 5750.73±460.19 vs 3256.87±461.15, $P<0.01$). There was no significant difference in the expressions of HMGB1 and AP1 among the para-PVN tissue and the PVN in the control group and the para-PVN tissue in the experimental group (fig 6,7).

The levels of IL-1β in the PVN were examined by WB 72 hours after injury, which were significantly higher in the experimental group than that in the control group (0.80±0.03 vs 0.58±0.02, $P<0.01$) (fig 8).

3.5 HMGB1 promoted microglia activation and increased the expression of AP1 and IL-1β

When compared with microglia in the control group, synapses of most microglia were significantly decreased and shortened in the HMGB1 group. Cell bodies of microglia were also larger in the HMGB1 group than those in the control group, showing the activation of microglia after HMGB1 treatment (fig 9 A B) [52,53]. It was found that the ratio of activated microglia to the total number of cells in the HMGB1 group was higher than that in the control group (74.70% vs 24.52%, $P<0.001$) (fig 9C).

Results from RT-qPCR showed that after treatment with HMGB1 for 24 hours, the gene expression of AP1 and IL-1β in the HMGB1 group increased significantly compared with those in the control group (fig 10 A B). The protein expressions of AP1 and IL-1β were respectively examined by WB (Fig 10 C D) and ELISA (Fig 10 E), which is consistant with those of RT-qPCR.

3.6 Stereotactic injection of HMGB1 inhibitor or HMGB1 altered the expression of AP1 and IL-1β in the PVN.

At 72 hours after stroke or sham surgery, the expressions of AP1 and IL-1β in the PVN of rats were detected by WB. The results showed that the expressions of AP1 and IL-1β in the sham+HMGB1 group increased significantly compared with those of the sham+NS group. The expressions of AP1 and IL-1β in the DAI+Anti-HMGB1 group were lower than those in the DAI+NS group (fig 11).

3.7 Stereotactic injection of HMGB1 inhibitor or HMGB1 altered sympathetic excitability

The levels of MAP (112.47±0.94 mmHg vs 105.36±1.16 mmHg, P<0.001) and serum CA (321.78±14.47 ng/ml vs 293.78±11.52 ng/ml, P<0.05) increased significantly, while SDNN (5.55±0.08 ms vs 6.12±0.19 ms, P<0.001) decreased significantly in the sham+HMGB1 group, compared with those in the sham+NS group. However, the levels of MAP (107.98±1.15 vs 114.40±0.91, P<0.001) and CA (293.24±11.76 ng/ml vs 320.95±7.96 ng/ml, P<0.05) decreased significantly, and SDNN (5.79±0.05 ms vs 5.21±0.07 ms, P<0.001) increased significantly in the DAI+Anti-HMGB1 group, compared with those in the DAI+NS group (fig 12).

Discussion

Sympathetic hyperactivity after TBI is a serious clinical problem, while the specific pathological mechanism remains unraveled. Although studies have shown that the secretion of IL-1β by microglia in PVN might promote sympathetic hyperactivity [16, 23], the specific molecular mechanism of the secretion of IL-1β by microglia has not been fully revealed. We studied the relationship between the formation of NETs in the PVN and sympathoexcitation after TBI and verified that HMGB1/AP1 pathway might be involved in the development of sympathoexcitation by *in vivo* and *in vitro* experiments. We found that there were a large number of NETs in the PVN after DAI, which could activate microglia and promote the release of IL-1β through HMGB1/AP1 pathway, ultimately contributing to the occurrence of sympathoexcitation.

Clinically, sympathoexcitation after TBI generally occurs 48 hours to 2 weeks after injury and lasts for up to several months [5, 24–26]. We found that 72 hours after injury was the best observation time point for sympathoexcitation in rats [20]. At 72 hours after DAI, the formation level of NETs in PVN of the DAI group was higher than that in para-PVN tissues of the DAI group, while no NETs formation was found in PVN and para-PVN tissue in the control group. Some studies have shown that central granulocytes can penetrate the blood brain barrier into cerebrospinal fluid and brain tissues after trauma [8, 27]. In addition, Zhang B et al. found that neutrophil staining was observed in ventral side of the hypothalamus, periventricular region, meningeal, hemispheric union, small and large vessels of brain stem and specific brain structure, including PVN after brain injury [28]. Therefore, we tend to believe that a large number of central granulocytes infiltrate into PVN and form NETs after DAI.

It is widely accepted that the main function of microglia is to phagocytize small cell fragments in the process of neuronal development or damage repair. In recent years, studies have found that microglia possesses various important functions [29]. Microglia can be divided into resting state and activated state. Resting microglia use its processes to continuously detect virus, bacterial infection, tissue damage, cell debris, etc., so as to ensure the homeostasis and safety of the internal environment of the central nervous system [30]. After external stimulation, the resting microglia's cell body swelled along with their decreased processes, and gradually transformed into an activated state [31, 32]. It has been found that in adult Still disease, NETs can promote the activation of macrophages [23]. Microglia are regarded as macrophages in the central nervous system [33], so we infer that NETs could also activate microglia. In our experiment, we found that there were many processes and branches in the resting microglia cells. After HMGB1 treatment, one of the components of NETs, the processes of the microglia were shortened and decreased, and the cell body swelled, which confirmed our inference.

HMGB1 is an agonist ligand of RAGE receptor [34, 35], which has been found to be related to inflammatory response, immune response, cardiovascular disease and other pathological states [35]. RAGE is a pattern recognition receptor on the membrane of microglia and other cells, which can further promote the expression of AP1 [13], and mediate the inflammatory response in microglia [36, 37]. In addition, studies have also shown that AP1, a transcription factor, is closely related to the expression of inflammatory cytokines such as IL-1β [14, 15]. Therefore, we further examined the mRNA and protein expression levels of AP1 and IL-1β in microglia after HMGB1 administration. The results showed that changes in the expression of AP1 were consistent at the levels of transcription and translation, and so was IL-1β. This further confirmed that HMGB1 may activate the RAGE receptor on the surface of microglia. As a result, the expression of AP1 was increased, which contributed to the activation of microglia and secretion of IL-1β. After TBI, IL-1β is the key cytokine of inflammatory response. It can also regulate the function of excitatory or inhibitory postsynaptic receptors, as well as the expression level of their corresponding transmitters, thus regulating sympathetic excitability [16]. For example, IL-1β can directly act on neurons and their synapses, increase the release of glutamate transmitters and the activity of AMPA receptors, promoting the signal transmission of fast excitatory synapses in the central nervous system [17]. Additionally, studies on the pathogenesis of salt-dependent hypertension also found that IL-1β in PVN plays an important role in sympathoexcitation [18].

In order to verify the role of HMGB1/AP1 pathway in PSH after TBI, stereotactic injection of HMGB1 recombinant protein or HMGB1 inhibitor (anti-HMGB1) into PVN was performed. We found that the expressions of AP1 and IL-1β increased significantly in the sham+HMGB1 group compared with those in the sham+NS group. Compared with DAI + NS group, the expressions of AP1 and IL-1β in the DAI+Anti-HMGB1 group decreased significantly. Zhou and Zhang et al found that the down-regulation of HMGB1 receptor in mouse brain tissue could decrease the expression level of AP1, and HMGB1 could significantly increase the expression level of AP1 in cells [38, 39], which was coherent with our results. Wei et al found that the expression of AP1 in brain tissue could be upregulated 6 hours after brain injuries such as cerebral hemorrhage, accompanied by the increase of inflammatory factors such as IL-1β, while inhibition of AP1 expression can reduce the expression of IL-1β and other inflammatory factors [40]. Our results

also confirm this viewpoint. We also tested and analyzed the main indicators of sympathetic excitability, including HRV, MAP and serum CA content. We found that HMGB1 could significantly promote sympathoexcitation, while anti-HMGB1 could attenuate the sympathoexcitability after DAI. Interference with the activation of RAGE receptor by siHMGB1 in brain tissue can attenuate neuroinflammation and the consequent changes of systolic blood pressure of sympathetic vessels [41]. The expression of HMGB1 was also high in the PVN of spontaneously hypertensive rats with sympathoexcitation [10]. The above results further support the conclusion that HMGB1 in PVN activates RAGE receptor on microglia to mediate microglial activation through AP1, and then increases the secretion of IL-1β, finally promoting the development of sympathoexcitation.

There are also some limitations in our research. First of all, animal or cell models cannot fully reflect various pathophysiological and molecular pathways in the human body. Subsequent clinical trials in humans will make breakthroughs in the pathogenesis of sympathoexcitation after TBI. Secondly, we focused mainly on the intervention of HMGB1 but not on AP1. The direct effect of HMGB1 on RAGE receptors is in need of further explored. These limitations will be further refined in subsequent experimental studies.

Conclusion

It is the first time to propose that NETs in the PVN may cause sympathoexcitation by activating microglia via HMGB1/AP1 pathway after TBI. Possible molecular mechanisms of microglial activation were explored. Our findings will help elucidate the molecular mechanisms of sympathoexcitation after TBI and provide a new therapeutic target for clinical treatment.

Abbreviations

Abbreviation	Full Name
NETs	Neutrophil Extracellular Traps
HMGB1	High-Mobility Group Box 1
TBI	Traumatic Brain Injury
AP1	Activator Protein 1
PSH	Paroxysmal Sympathetic Hyperactivity
IL-1β	Interleukin 1β
β-APP	β-amyloid Precursor Protein
CitH3	Citrullinate Histone H3
MPO	Myeloperoxidase
PVN	Paraventricular Nucleus
GCS	Glasgow Coma Scale
DAI	Diffuse Axonal Injury
CNS	Central Nervous System
NE	Neutrophil Elastase
RAGE	Receptor for Advanced Glycation End Products
NMDA	N-Methyl-D-aspartic Acid
GABA	Gamma-Amino Butyric Acid
WB	Western Blot
qPCR	Quantitative Real-Time PCR
CA	Catecholamine
HRV	Heart Rate Variability
SDNN	Standard Deviation of Normal-to-Normal RR Intervals

Declarations

Acknowledgements

Not applicable.

Ethics approval and consent to participate

All experimental operations strictly abided by the Guide for the Care and Use of Laboratory Animals published by US National Institutes of Health (NIH publication No.85-23, revised 1996) and were approved by Animal Care and Use Committee of the Naval Medical University.

Consent for publication

Not applicable.

Competing interests

The authors declare that they have no competing interests.

Availability of data and materials

The datasets generated during and/or analyzed during the current study are available from the corresponding author on reasonable request.

Authors' contributions

△Kaixin Zhu, Xiaoxiang Hou, and Xiaolin Qu contributed equally to this work.

Author details

[1]Department of neurosurgery, Changzheng Hospital, Naval Medical University, Shanghai, China. [2] Department of Neurosurgery, The First Naval Hospital of Southern Theater Command, Guangdong, China.

Funding

This work was supported by the National Natural Science Foundation of China (NSFC) [grant numbers 81901242], Chenguang Project of Shanghai [Danfeng Zhang, grant numbers 19CG39] and Shanghai Yang Fan Project (Danfeng Zhang, grant numbers 19YF1447900].

References

1. Zeng, Z., et al., *Modulation of autophagy in traumatic brain injury.* 2020. **235**(3): p. 1973–1985.
2. Thomas, A., B.J.A.j.o.p.m. Greenwald, and rehabilitation, *Paroxysmal Sympathetic Hyperactivity and Clinical Considerations for Patients With Acquired Brain Injuries: A Narrative Review*. 2019. **98**(1): p. 65–72.
3. Khalid, F., et al., *Autonomic dysfunction following traumatic brain injury: translational insights*. 2019. **47**(5): p. E8.
4. Baguley, I., et al., *Paroxysmal sympathetic hyperactivity after acquired brain injury: consensus on conceptual definition, nomenclature, and diagnostic criteria*. 2014. **31**(17): p. 1515–20.

5. Meyfroidt, G., I. Baguley, and D.J.T.L.N. Menon, *Paroxysmal sympathetic hyperactivity: the storm after acute brain injury.* 2017. **16**(9): p. 721–729.
6. Compton, E.J.T.N.c.o.N.A., *Paroxysmal Sympathetic Hyperactivity Syndrome Following Traumatic Brain Injury.* 2018. **53**(3): p. 459–467.
7. Koba, S., et al., *Sympathoexcitation by hypothalamic paraventricular nucleus neurons projecting to the rostral ventrolateral medulla*. 2018. **596**(19): p. 4581–4595.
8. Roth, T., et al., *Transcranial amelioration of inflammation and cell death after brain injury.* 2014. **505**(7482): p. 223–8.
9. Papayannopoulos, V.J.N.r.I., *Neutrophil extracellular traps in immunity and disease.* 2018. **18**(2): p. 134–147.
10. Masson, G., et al., *Aerobic training normalizes autonomic dysfunction, HMGB1 content, microglia activation and inflammation in hypothalamic paraventricular nucleus of SHR*. 2015. **309**(7): p. H1115-22.
11. Gao, T., et al., *Expression of HMGB1 and RAGE in rat and human brains after traumatic brain injury*. The journal of trauma and acute care surgery, 2012. **72**(3): p. 643–9.
12. Dwir, D., et al., *MMP9/RAGE pathway overactivation mediates redox dysregulation and neuroinflammation, leading to inhibitory/excitatory imbalance: a reverse translation study in schizophrenia patients*. Molecular psychiatry, 2020. **25**(11): p. 2889–2904.
13. Adamopoulos, C., et al., *Advanced glycation end products upregulate lysyl oxidase and endothelin-1 in human aortic endothelial cells via parallel activation of ERK1/2-NF-κB and JNK-AP-1 signaling pathways*. 2016. **73**(8): p. 1685–98.
14. Kim, J., et al., *IL-1β and IL-6 activate inflammatory responses of astrocytes against Naegleria fowleri infection via the modulation of MAPKs and AP-1*. 2013. **35**: p. 120–128.
15. Lopez-Bergami, P., E. Lau, and Z.J.N.r.C. Ronai, *Emerging roles of ATF2 and the dynamic AP1 network in cancer*. 2010. **10**(1): p. 65–76.
16. Wang, Y., et al., *Microglial Mincle receptor in the PVN contributes to sympathetic hyperactivity in acute myocardial infarction rat*. 2019. **23**(1): p. 112–125.
17. Yan, X., et al., *Interleukin-1beta released by microglia initiates the enhanced glutamatergic activity in the spinal dorsal horn during paclitaxel-associated acute pain syndrome*. 2019. **67**(3): p. 482–497.
18. Qi, J., et al., *Targeting Interleukin-1 beta to Suppress Sympathoexcitation in Hypothalamic Paraventricular Nucleus in Dahl Salt-Sensitive Hypertensive Rats*. 2016. **16**(3): p. 298–306.
19. Zhu, K., et al., *NETs Lead to Sympathetic Hyperactivity After Traumatic Brain Injury Through the LL37-Hippo/MST1 Pathway.* 2021. **15**: p. 621477.
20. Chen, J., et al., *Effect of oxidative stress in rostral ventrolateral medulla on sympathetic hyperactivity after traumatic brain injury*. 2019. **50**(2): p. 1972–1980.
21. Baguley, I., et al., *Gabapentin in the management of dysautonomia following severe traumatic brain injury: a case series*. 2007. **78**(5): p. 539–41.

22. Albrengues, J., et al., *Neutrophil extracellular traps produced during inflammation awaken dormant cancer cells in mice*. 2018. **361**(6409).
23. Silva, T., et al., *Minocycline alters expression of inflammatory markers in autonomic brain areas and ventilatory responses induced by acute hypoxia*. 2018. **103**(6): p. 884–895.
24. Lv, L., et al., *Prognostic influence and magnetic resonance imaging findings in paroxysmal sympathetic hyperactivity after severe traumatic brain injury*. 2010. **27**(11): p. 1945–50.
25. Lv, L., et al., *Risk factors related to dysautonomia after severe traumatic brain injury*. 2011. **71**(3): p. 538–42.
26. Lv, L., et al., *Hyperbaric oxygen therapy in the management of paroxysmal sympathetic hyperactivity after severe traumatic brain injury: a report of 6 cases*. 2011. **92**(9): p. 1515–8.
27. Liao, Y., et al., *Oxidative burst of circulating neutrophils following traumatic brain injury in human.* 2013. **8**(7): p. e68963.
28. Zhang, B., et al., *Splenectomy protects experimental rats from cerebral damage after stroke due to anti-inflammatory effects*. 2013. **126**(12): p. 2354–60.
29. Prinz, M., S. Jung, and J.J.C. Priller, *Microglia Biology: One Century of Evolving Concepts.* 2019. **179**(2): p. 292–311.
30. Nimmerjahn, A., F. Kirchhoff, and F.J.S. Helmchen, *Resting microglial cells are highly dynamic surveillants of brain parenchyma in vivo.* 2005. **308**(5726): p. 1314–8.
31. Loane, D. and A.J.E.n. Kumar, *Microglia in the TBI brain: The good, the bad, and the dysregulated.* 2016: p. 316-327.
32. Tang, Y. and W.J.M.n. Le, *Differential Roles of M1 and M2 Microglia in Neurodegenerative Diseases.* 2016. **53**(2): p. 1181-1194.
33. Gosselin, D., et al., *An environment-dependent transcriptional network specifies human microglia identity.* 2017. **356**(6344).
34. Scaffidi, P., T. Misteli, and M.J.N. Bianchi, *Release of chromatin protein HMGB1 by necrotic cells triggers inflammation*. 2002. **418**(6894): p. 191–5.
35. Bangert, A., et al., *Critical role of RAGE and HMGB1 in inflammatory heart disease*. 2016. **113**(2): p. E155-64.
36. Gao, T., et al., *Expression of HMGB1 and RAGE in rat and human brains after traumatic brain injury*. 2012. **72**(3): p. 643–9.
37. Dwir, D., et al., *MMP9/RAGE pathway overactivation mediates redox dysregulation and neuroinflammation, leading to inhibitory/excitatory imbalance: a reverse translation study in schizophrenia patients*. 2020. **25**(11): p. 2889–2904.
38. Zhou, Z., et al., *Geniposidic acid ameliorates spatial learning and memory deficits and alleviates neuroinflammation via inhibiting HMGB-1 and downregulating TLR4/2 signaling pathway in APP/PS1 mice*. 2020. **869**: p. 172857.

39. Zhang, Z., et al., *[HMGB1-mediated activation of TLR4 signaling in hepatic stellate cells]*. 2012. **20**(8): p. 581–4.
40. Wei, C., et al., *Inhibition of activator protein 1 attenuates neuroinflammation and brain injury after experimental intracerebral hemorrhage*. 2019. **25**(10): p. 1182–1188.
41. Zhang, S., et al., *HMGB1/RAGE axis mediates stress-induced RVLM neuroinflammation in mice via impairing mitophagy flux in microglia*. 2020. **17**(1): p. 15.

Figures

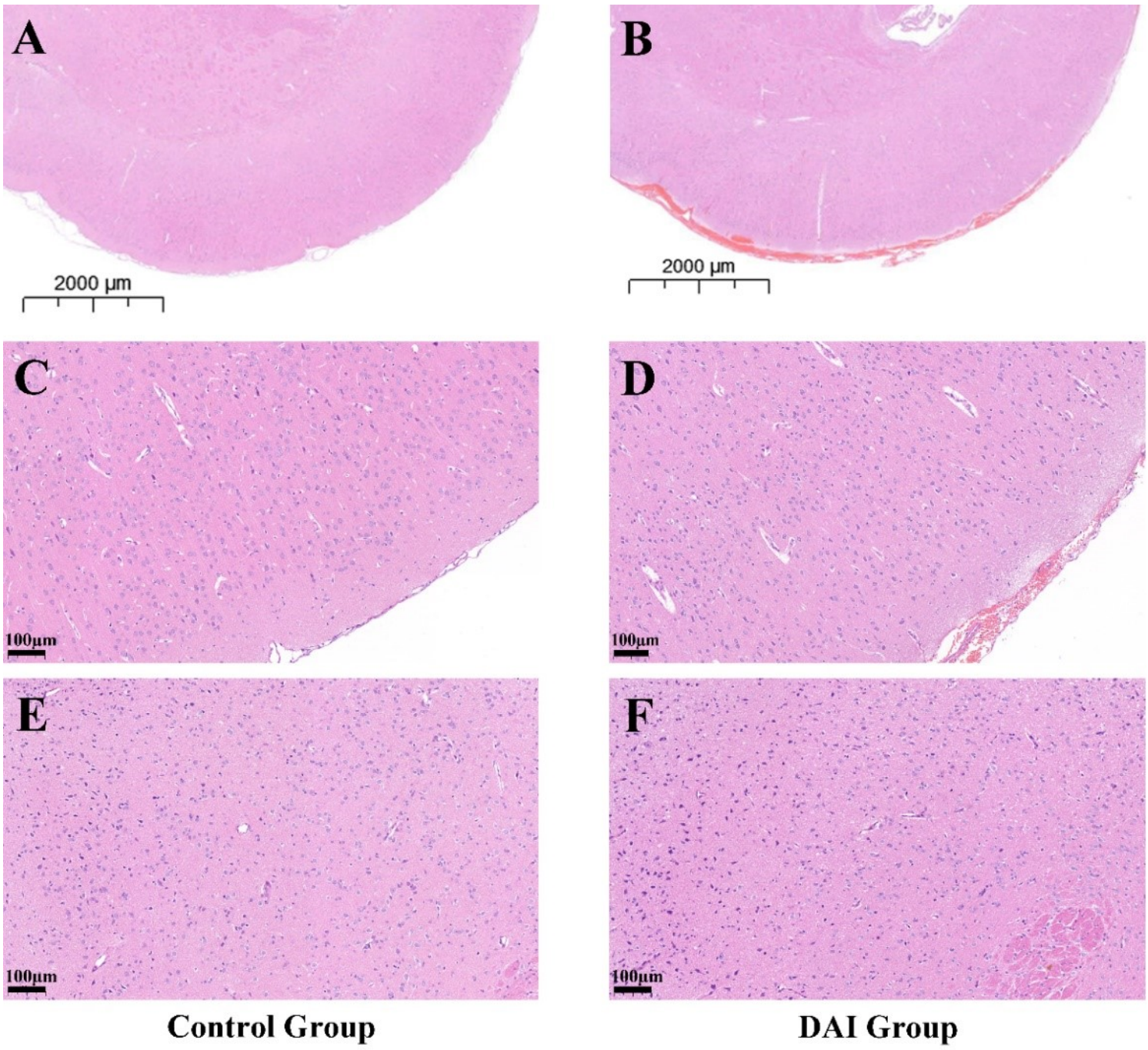

Figure 1

HE staining of brain tissue after DAI. A, C, E: there was no abnormality in brain tissue in the control group. B. D: in the DAI group, a large number of blood cells were found in subarachnoid space, and the perivascular space was significantly enlarged. F: nuclear pyknosis, deep staining and morphological changes were found in a large number of cells in the hypothalamus. A, B: scale bar, 2000μm, C-F: scale bar, 100μm.

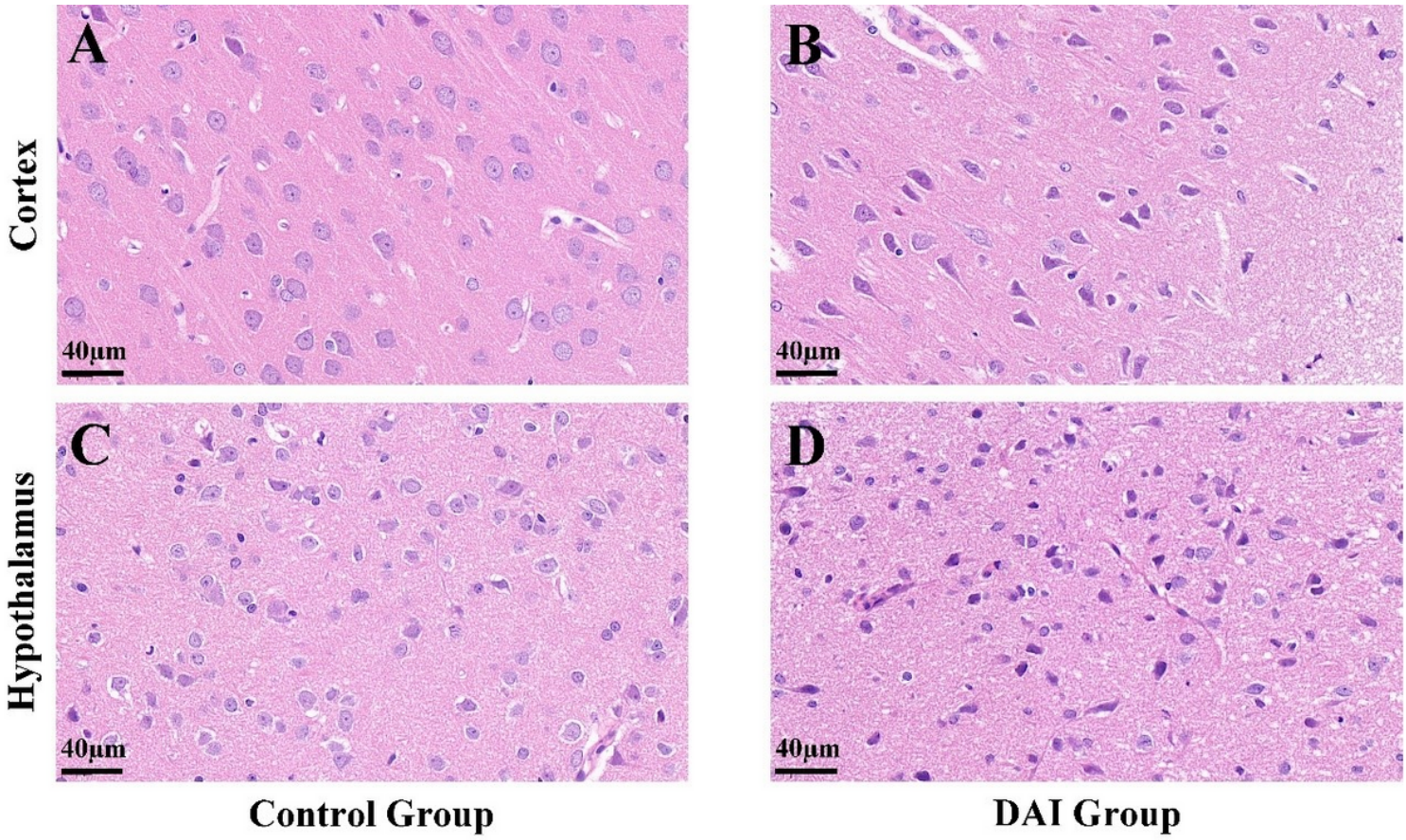

Figure 2

HE staining of cortex and hypothalamus was shown. A, C: there was no abnormality in brain tissue in the control group. B, D: the space around cells increased. Nuclear pyknosis, deepening of staining and morphological changes were found in a large number of cells in the DAI group. scale bar: 40μm.

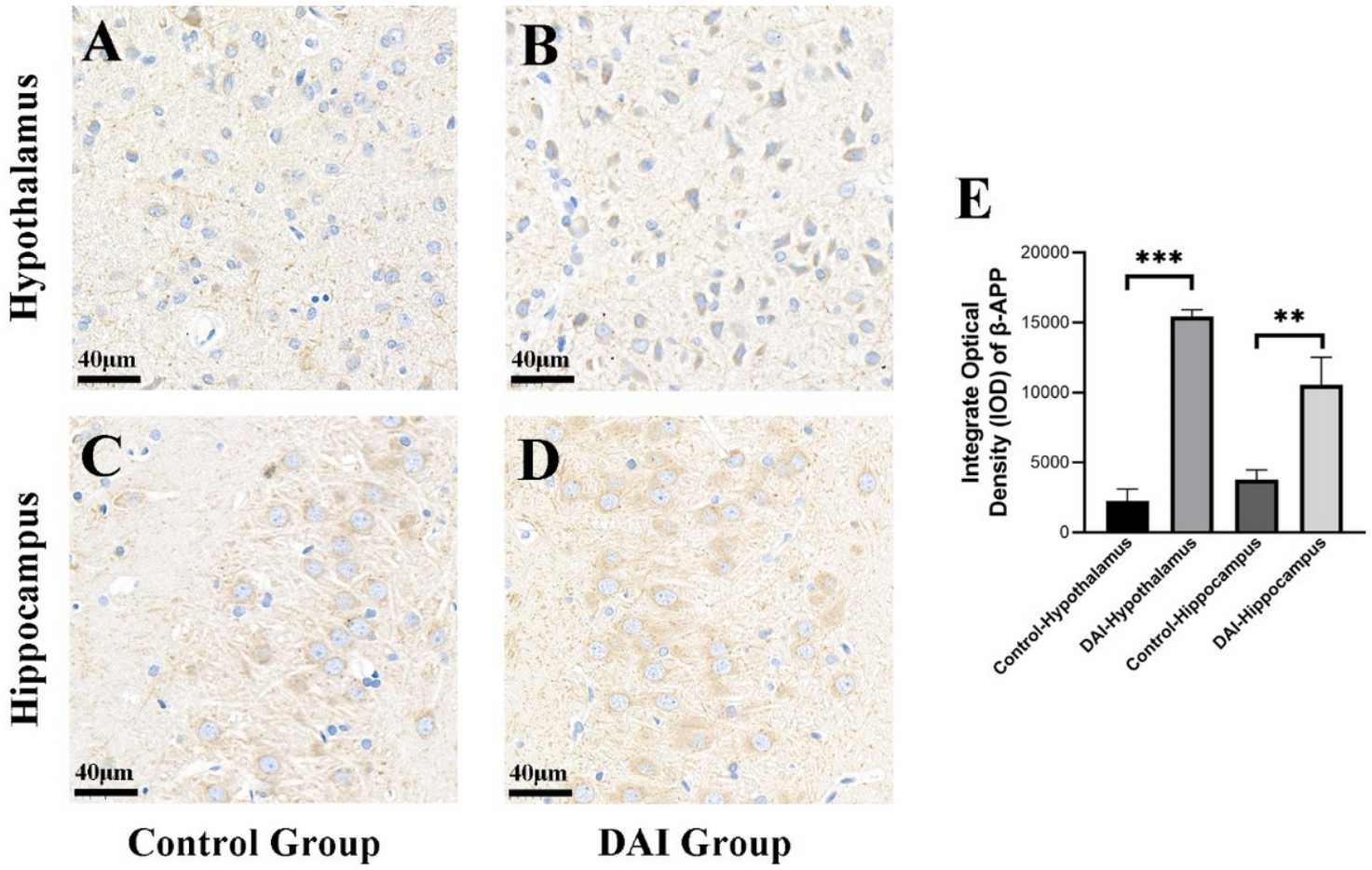

Figure 3

In the DAI group, the expression of β-APP in the hypothalamus and hippocampus increased significantly, and some nuclei were pyknotic and deformed. A-D: representative immunochemistry of β-APP on hypothalamus and hippocampus sections obtained from rats in the DAI or control group. E: results of IOD showed that the expression of β-App in the DAI group was higher than that in the control group. * P<0.05, ** P<0.01, *** P<0.001, Scale bar: 40μm

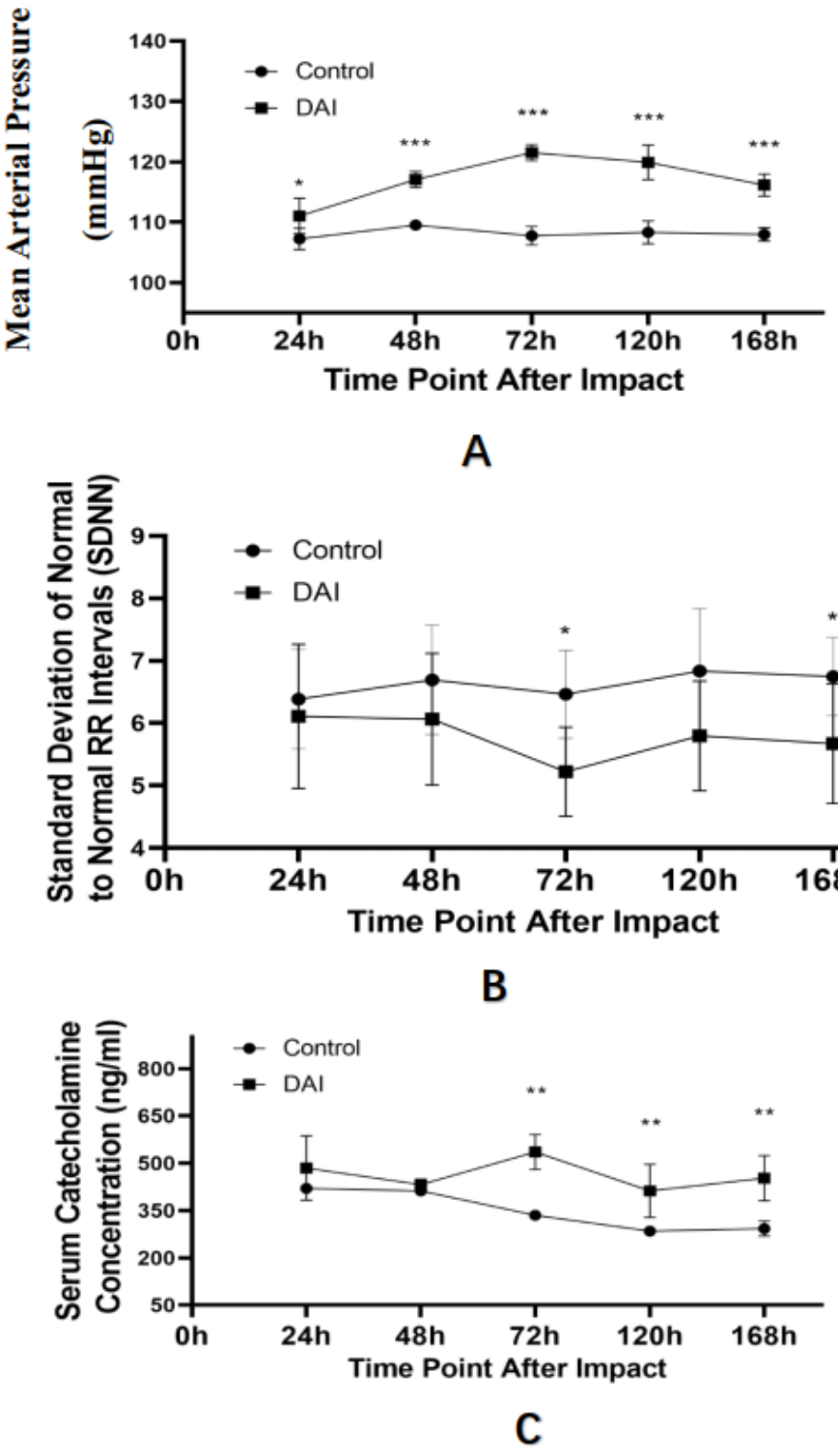

Figure 4

The analysis of MAP, SDNN, serum CA concentration. A: MAP of rats in the DAI group was higher than that of the control group, and reached the peak at 72 hours after injury; MAP of the control group was stable at all times. B: SDNN of rats in the DAI group showed a downward trend after DAI attack and reached the lowest value at 72 hours; the SDNN of rats in the control group was stable at all times. C: the concentration of serum CA (ng/ml) in the DAI group peaked at 72 hours after injury; the content of serum

CA in the control group began to decline at 48 hours after the sham operation, and the overall trend was relatively stable. * P<0.05, ** P<0.01, *** P<0.001.

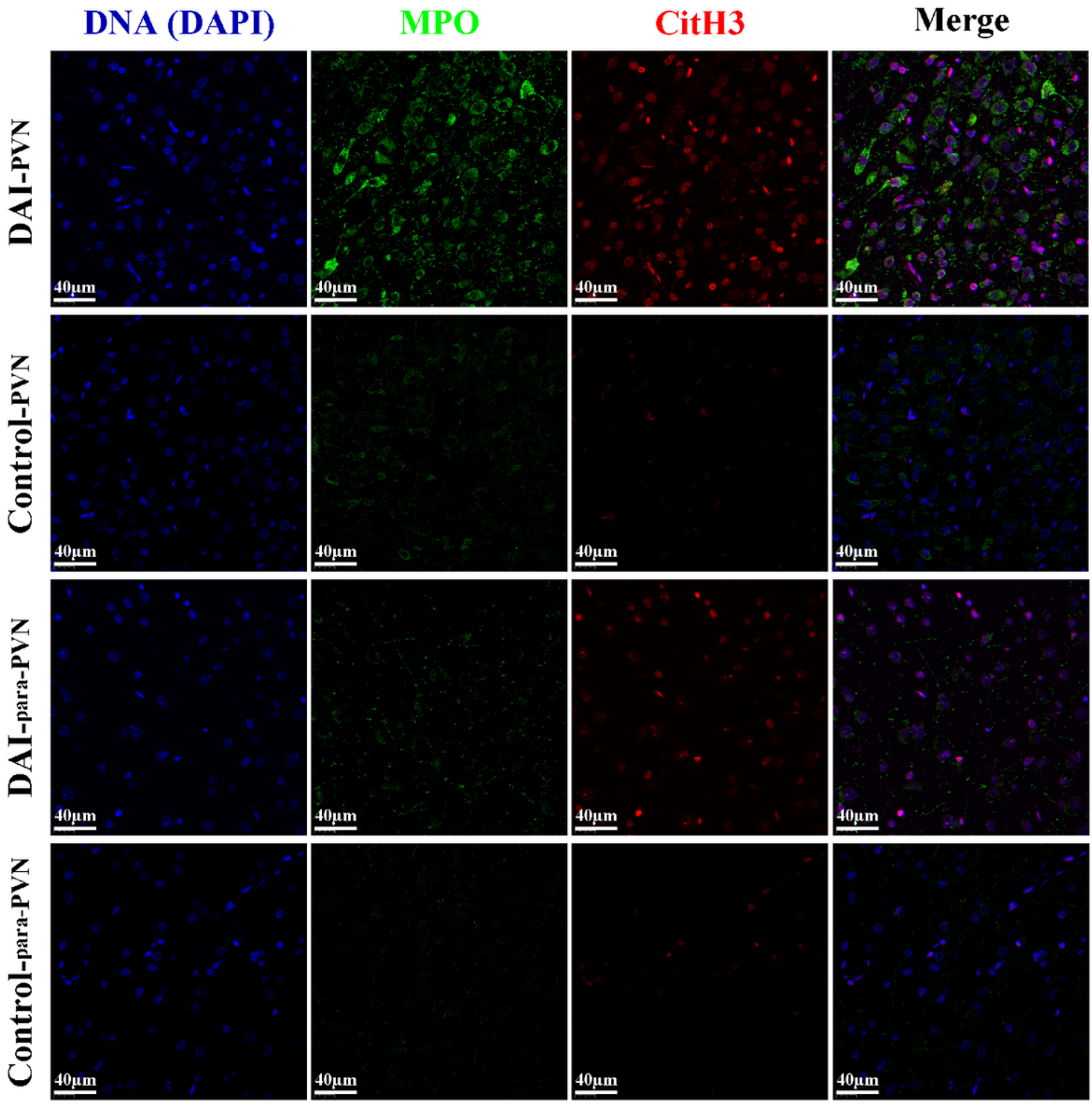

Figure 5

Representative double-staining immunofluorescence of CitH3 and MPO on brain sections of DAI rats. In DAI group, the levels of NETs in the PVN were higher than that in para-PVN tissue. In the control group, there was no formation of NETs within the PVN or in the pare-PVN tissue. Scale bar: 40μm.

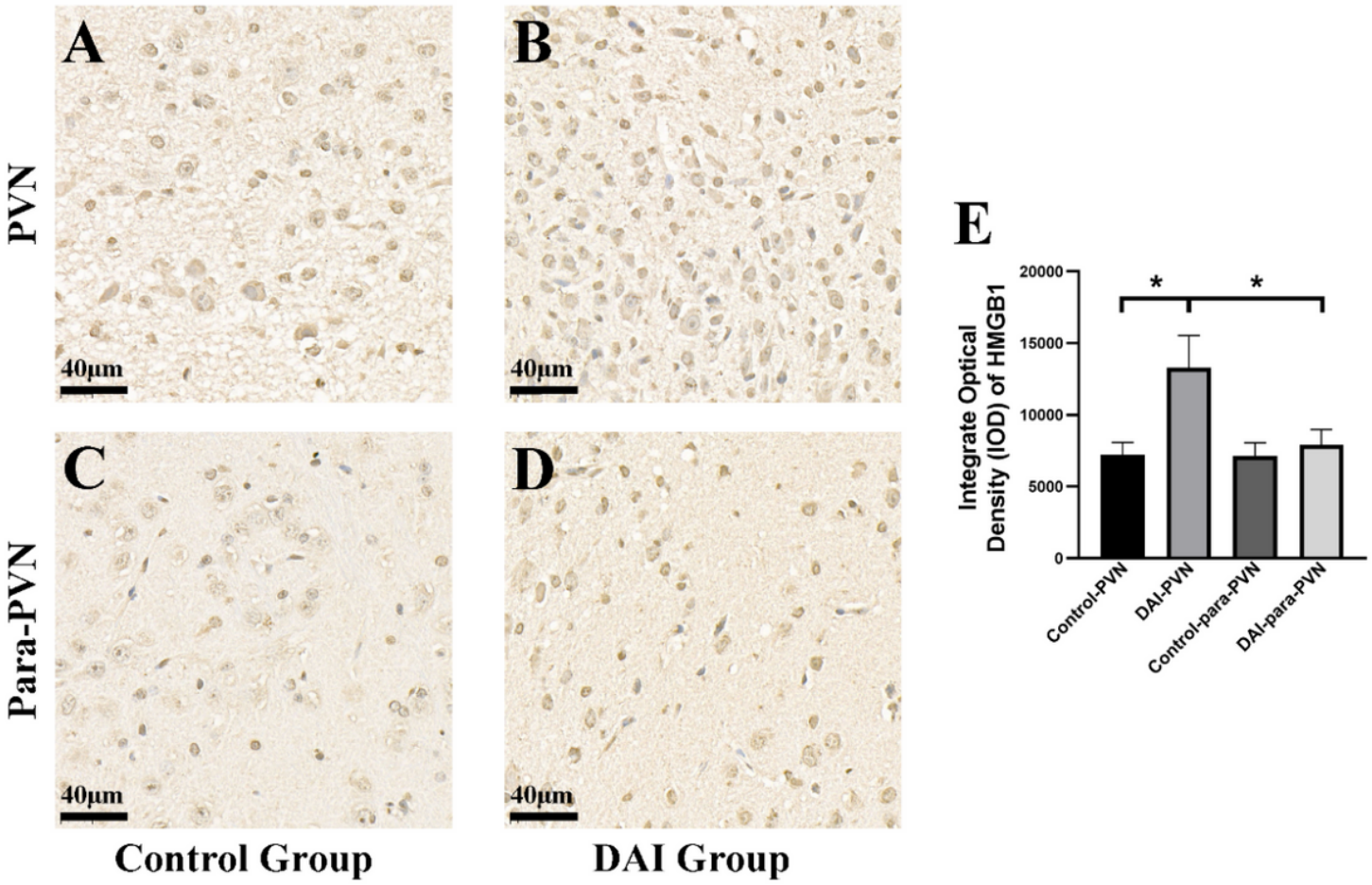

Figure 6

In the DAI group, the expression of HMGB1 in PVN was higher than that in para-PVN tissue, and there was no significant difference in the expression of HMGB1 among the para-PVN tissue and the PVN in the control group and the para-PVN tissue in the DAI group. A-D: representative immunochemistry of HMGB1 in the PVN and para-PVN of rats in DAI or control group. E: the IOD of immunochemistry of HMGB1. * P<0.05, ** P<0.01, *** P<0.001, Scale bar: 40μm

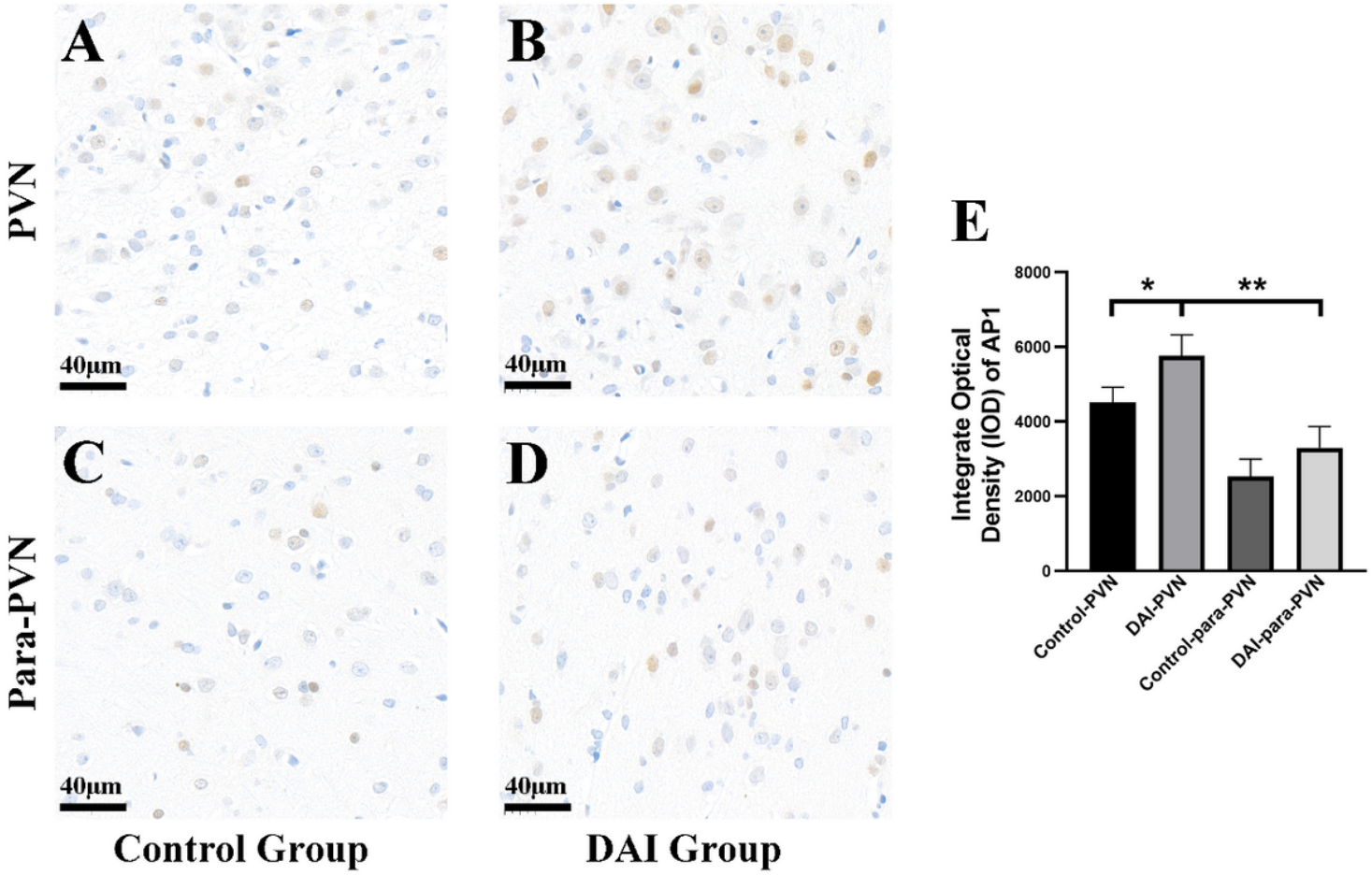

Figure 7

In DAI group, the expression of AP1 in PVN was higher than that in para-PVN tissue, and there was no significant difference in the expression of AP1 among the para-PVN tissue and the PVN in the control group and the para-PVN tissue in the DAI group. A-D: representative immunochemistry of AP1 in the PVN and para-PVN tissue of rats in the DAI or control group. E: the IOD of the immunochemistry of AP1. * P<0.05, ** P<0.01, *** P<0.001, Scale bar: 40μm

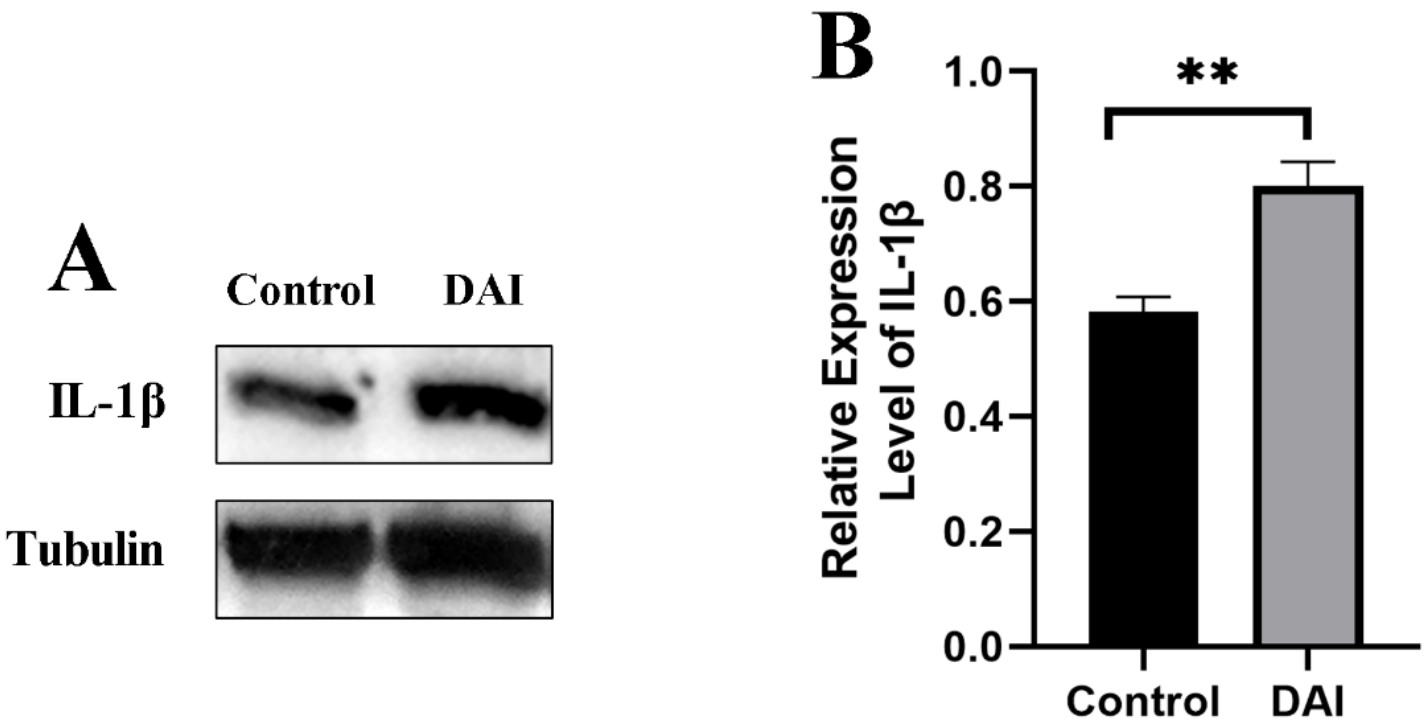

Figure 8

The levels of IL-1β in the DAI group were significantly higher than those in the control group. A: representative blots of IL-1β and Tubulin. B: densitometry quantification of IL-1β.

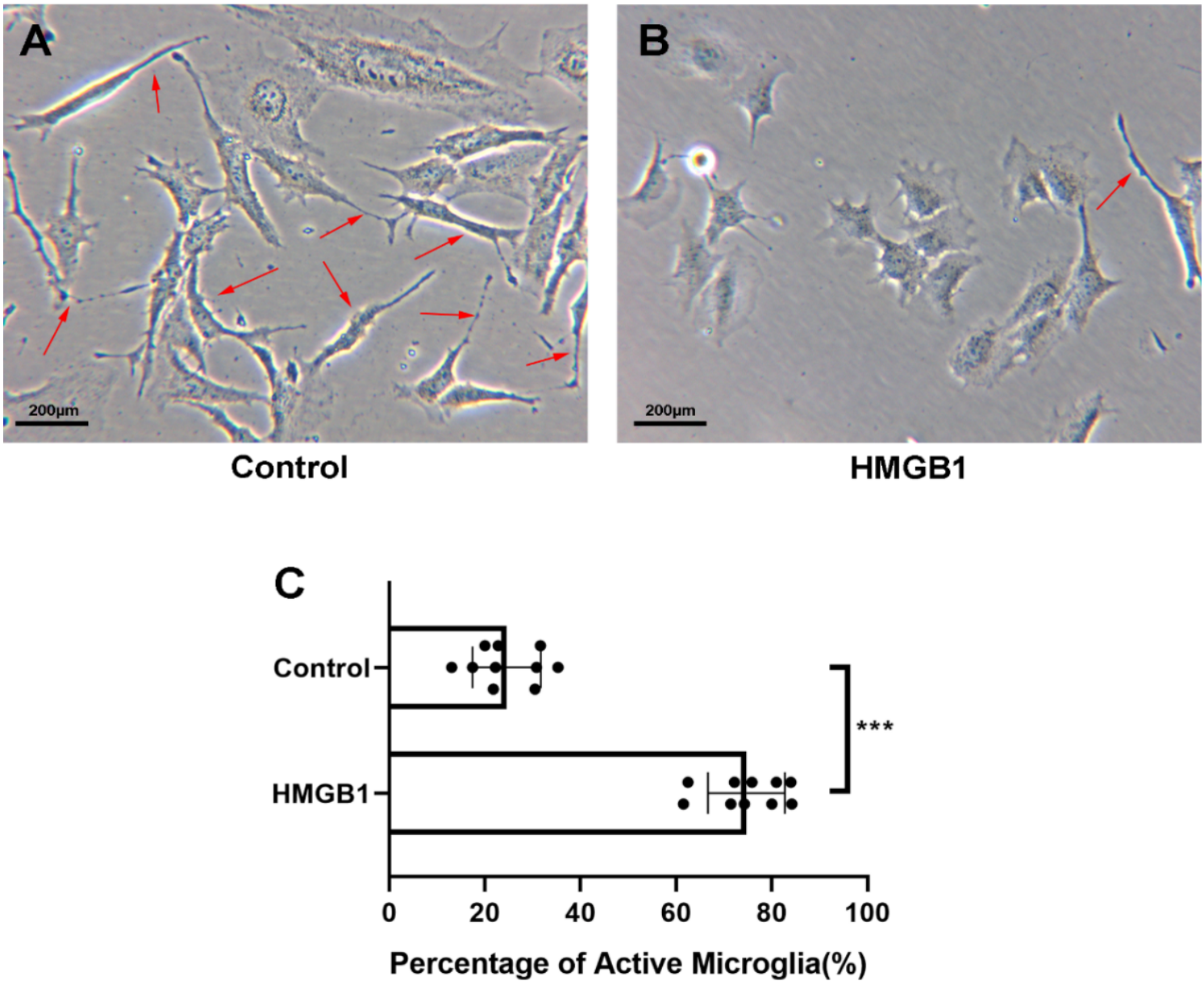

Figure 9

Activation of microglia after treatment with HMGB1. A: the resting state microglia had many synapses and small somas. B: activated microglia had fewer processes and larger somas. C: the ratio of active microglia in the HMGB1 group was higher than that in the control group. * P<0.05, ** P<0.01, *** P<0.001, Scale bar: 200μm.

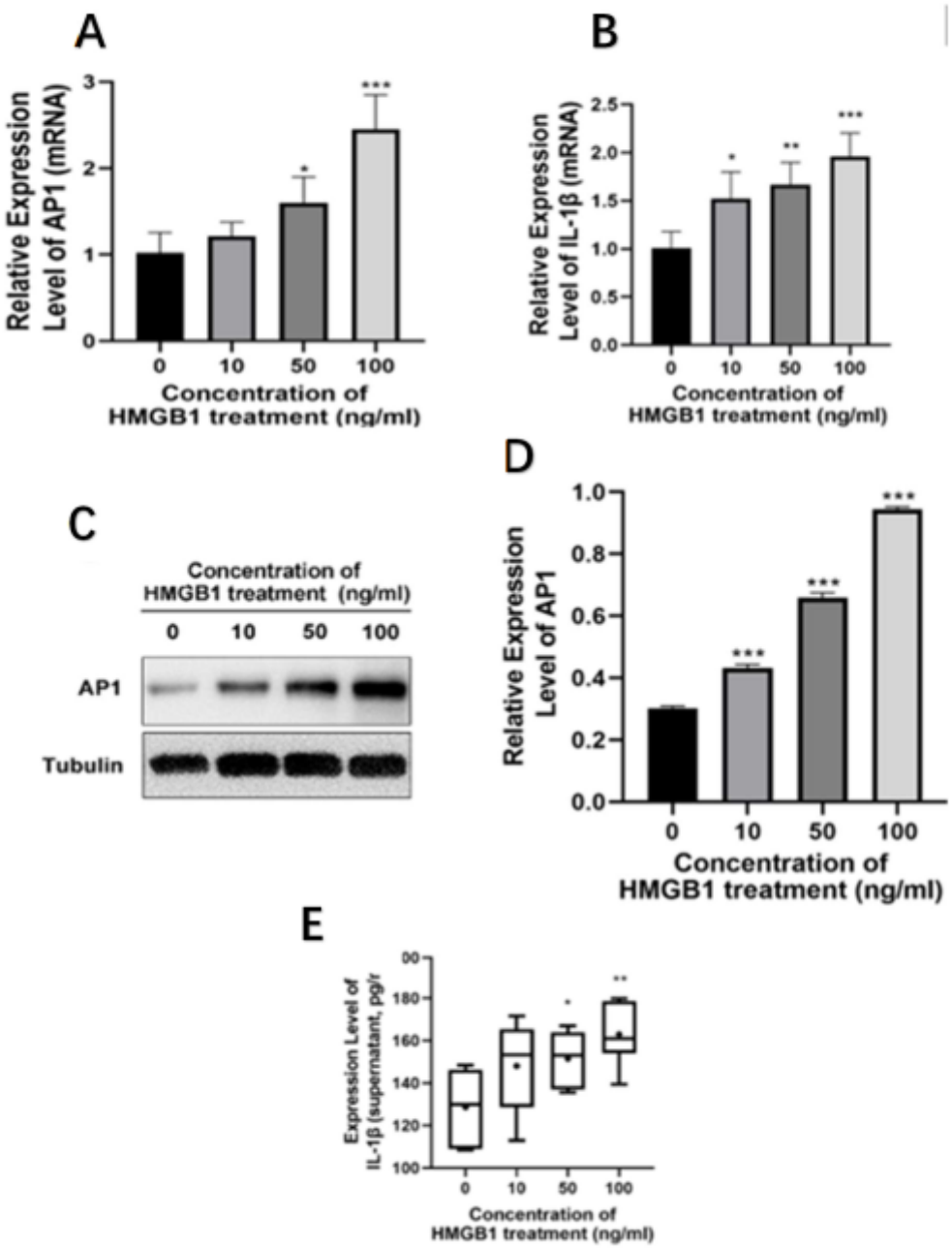

Figure 10

A, B: results from qPCR showed that the gene expression of AP1 and IL-1β in the HMGB1 group was higher than that in the control group. C, D: results of WB showed that the expression of AP1 in the HMGB1 group was higher than that in the control group. E: ELISA showed that the expression of IL-1β in the HMGB1 group was higher than that in the control group. * P<0.05 ** P<0.01 *** P<0.001

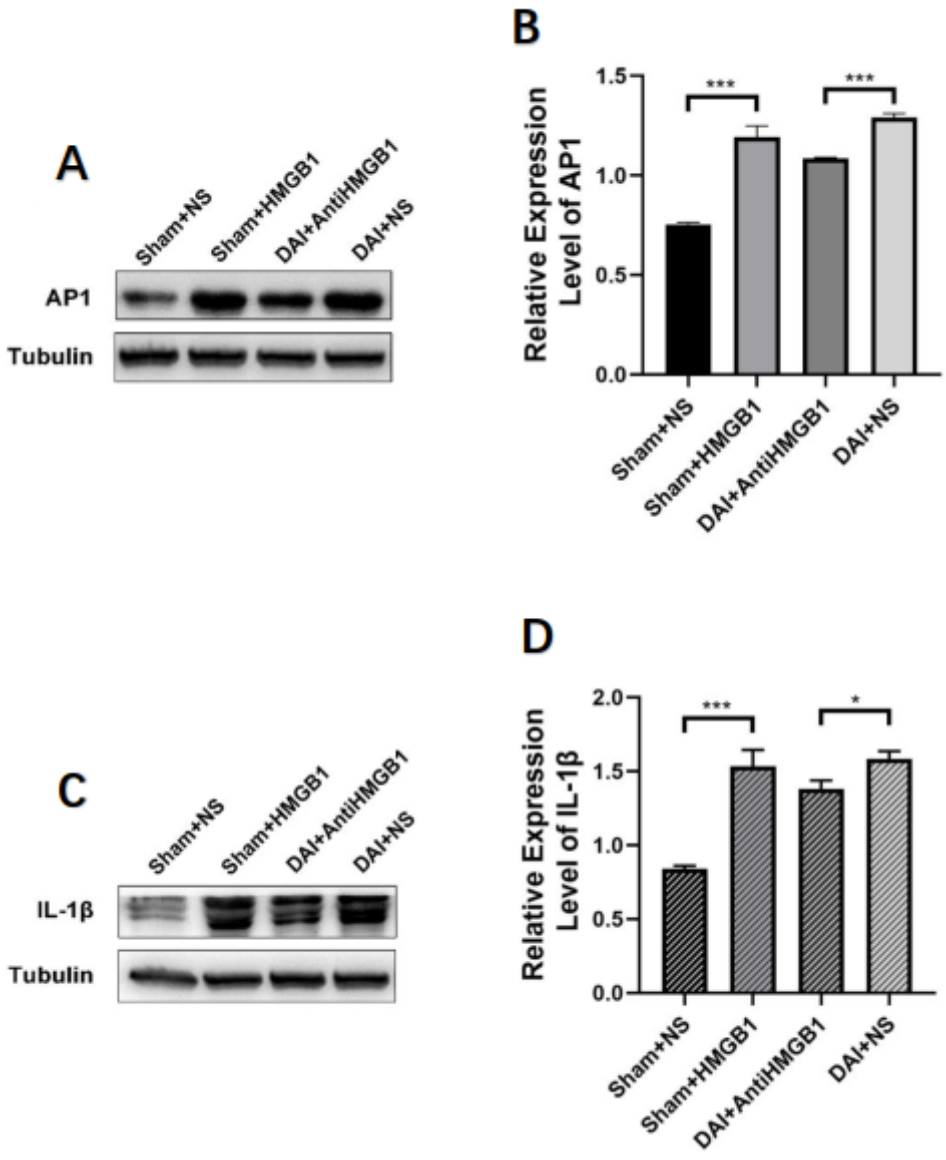

Figure 11

The expressions of AP1 and IL-1β in the sham+HMGB1 group increased significantly compared with those in the sham+NS group. The expressions of AP1 and IL-1β in the DAI+Anti-HMGB1 group were lower than those in the DAI+NS group. A, C: representative blots of AP1, IL-1β and Tubulin. B, D: densitometry quantification of AP1 and IL-1β. * P<0.05, ** P<0.01, *** P<0.001

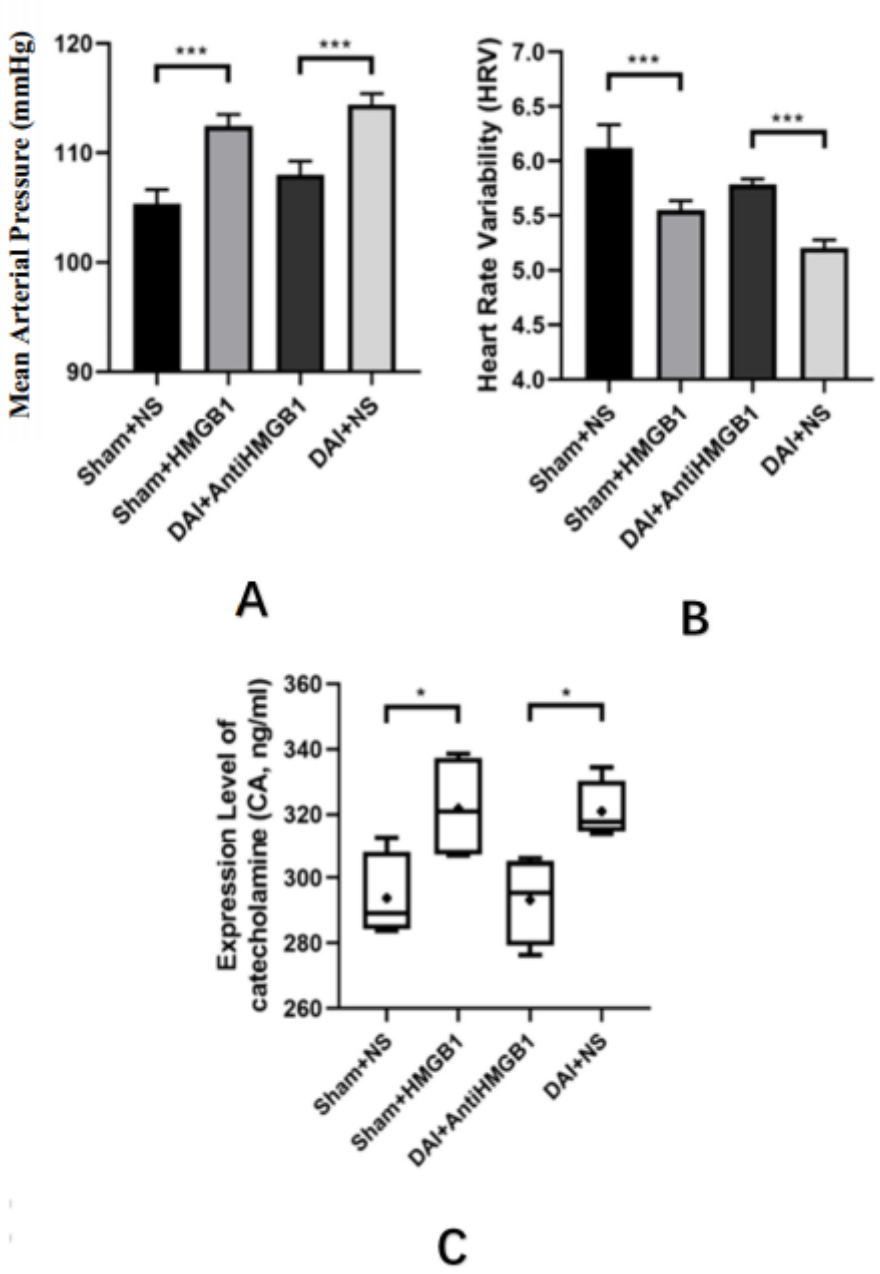

Figure 12

Stereotactic injection of HMGB1 inhibitor or HMGB1 altered sympathetic excitability. A, C: the levels of MAP and serum CA concentration in the sham+HMGB1 group were higher than those in the sham+NS group, and the levels of MAP and serum CA concentration in the DAI+Anti-HMGB1 group were lower than those in the DAI+NS group. B: HRV in the sham+HMGB1 group was lower than that in the sham+NS group, and HRV in the DAI+Anti-HMGB1 group was higher than that in the DAI+NS group. * $P<0.05$, ** $P<0.01$, *** $P<0.001$